ELSEVIER

Computer-Aided Design 37 (2005) 1370–1387

COMPUTER-AIDED DESIGN

www.elsevier.com/locate/cad

Constructing medial axis transform of extruded and revolved 3D objects with free-form boundaries

M. Ramanathan[1], B. Gurumoorthy*

Department of Mechanical Engineering, Centre of Product Design and Manufacturing, Indian Institute of Science, Bangalore 560 012, India

Received 1 May 2003; received in revised form 28 December 2004; accepted 25 January 2005

Abstract

This paper presents an algorithm for generating the Medial Axis Transform (MAT) of 3D objects with free form boundaries that are obtained by extrusion along a line or revolution about an axis. The algorithm proposed uses the exact representation of the part and generates an approximate rational spline description (to within a defined tolerance) of the MAT. The algorithm uses the 2D MAT of the profile being extruded or revolved to identify the limiting entities (junction points, seams and points of extremal maximum curvature) of the 3D MAT. It is shown that the MAT points of the profile face are sufficient to determine the topology and geometry of the MAT of this class of solids. The algorithm works for multiply-connected objects as well. Results of implementation are presented and use of the algorithm to handle general solids is discussed.

Keywords: Medial axis transform; Voronoi diagram; Skeleton; Free form boundaries

1. Introduction: medial axis transform

The Medial Axis Transform (MAT) was first introduced by Blum [1,2] to describe biological shape. It can be viewed as the locus of the center of a maximal ball as it rolls inside an object. Since its introduction, the MAT has found use in a wide variety of applications that primarily involve reasoning about geometry or shape. The MAT has been used in pattern analysis and image analysis [3,4], finite element mesh generation [5,6], mold design [7] and path planning [8], to name a few. There exists a bijective mapping between the MAT and object boundary [9] which means that for an object, there will be a unique MAT. Moreover, it is possible to reconstruct the object given its MAT [10]. The MAT can potentially be used as a representation scheme in geometric modelers, along with more popular schemes, such as constructive solid geometry (CSG) and boundary representation (B-rep) [11]. More importantly, dimensional reduction and topological equivalence make the MAT a simplified, abstract representation of the geometry. Since the MAT also provides details with respect to the symmetry of the object, it can be used in applications where this property is considered important.

The Medial Axis (MA), or skeleton of the set D, denoted $M(D)$, is defined as the locus of points inside D which lie at the centers of all closed balls (or disks in 2D) which are maximal in D, together with the limit points of this locus. A closed ball (or disk) is said to be *maximal* in a subset D of the 3D (or 2D) space if it is contained in D but is not a proper subset of any other ball (or disk) contained in D. The radius function of the MA of D is a continuous, real-valued function defined on $M(D)$ whose value at each point on the MA is equal to the radius of the associated maximal ball or disk. The medial axis transform (MAT) of D is the MA together with its associated radius function. Note that this definition of MAT is not restricted to R^3 and is applicable to metric space of any dimension.

The boundary and the corresponding MAT of an object is shown in Fig. 1. An important characteristic of the MAT is that it can be used to simplify the original object and still retain the original object's information. For instance, the two-dimensional MAT defines a unique, coordinate-system-

* Corresponding author. Tel.: +91 80 2293 2304; fax: +91 80 2360 0648.

E-mail address: bgm@mecheng.iisc.ernet.in (B. Gurumoorthy).

[1] Currently, Post-Doctoral Associate, Department of Computer Science, Technion, Israel.

0010-4485//$ - see front matter © 2005 Elsevier Ltd. All rights reserved.
doi:10.1016/j.cad.2005.01.006

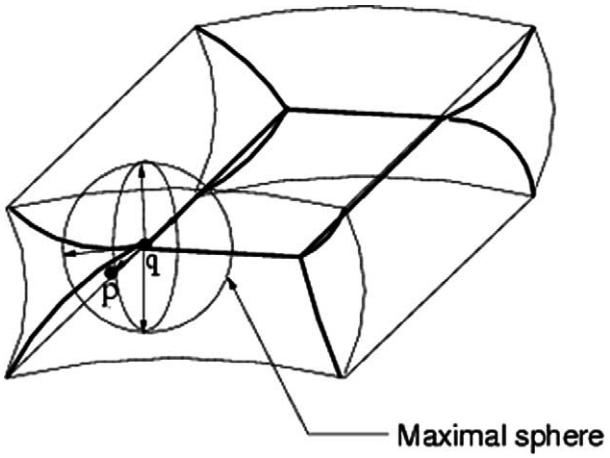

Fig. 1. Boundary and its medial axis.

independent decomposition of a planar shape into lines and the three dimensional MAT simplifies a solid model into a collection of surface patches. MAT of an object is therefore also called the *Skeleton* or *Symmetric axis* transform of a part/shape.

There have been several efforts reported for the construction of MAT for 3D objects. Most of these efforts focus on polyhedral objects. Very few algorithms that can handle free form entities have been reported. In general, obtaining a continuous description of MAT (in 2D or 3D) has proven to be difficult. Bisector surface, defined to be an equidistant surface between two surfaces, is an entity that can be used in constructing the MAT. However, a rational description or a closed-form rational representation is proven to be available only for certain special cases—between two rational space curves [20] and for CSG primitives in special configurations [19,22]. Bisector surface between two rational surfaces in R^3 is non-rational, in general [22]. Also, the bisector of simple geometries is not always simple. While the bisector of two lines in the plane is a line, the bisector of two skewed lines in R^3 is a hyperbolic paraboloid of one sheet [21]. Moreover, the post-processing involved in identifying valid bisectors and trimming them [15] have proven to be costly even in 2D and this has led to approaches based on tracing and intersection of normals [28]. In 3D, this has led to techniques based on discretisation, spatial decomposition and numerical tracing-most of them require formulation of differential equations and solving them, the exception being [24]. The discretisation based methods [13,14] discretise the domain in consideration into a point set. MAT is computed based on the idea that the circumspheres of the Delaunay triangulation of the point set approximate the maximal spheres. Clearly, an infinite point set is required to achieve this and this has led to a sparse distribution with adaptive refining method [13]. This procedure is not proven to be correct and gives only the topology information of the MAT and not the exact geometry. Optimization procedures have to be used to derive the exact geometry [14]. However, this has been shown to work only for implicit solid models. Spatial decomposition method using octree appears elegant, but could lead to high consumption of memory. It is shown to work for set-theoretic solid models [23] and polyhedral models [24,25]. However, the algorithm in [24] does not generate all medial surface patches and the algorithm in [25] generates approximate Voronoi graph for degenerate Voronoi diagrams.

Also, we are not aware of any such techniques for free-form solid models. Sherbrooke et al. [16,17] implemented a numerical tracing method using partial differential equations for constructing MAT for polyhedral objects. However, doubts have been raised about its numerical stability because of floating point arithmetic. It is shown that more accurate results can be obtained using exact arithmetic [18]. However, optimization methods are required to improve the speed because exact arithmetic has been proved to be very slow.

In general, algorithms that claim to handle free-form objects either discretise the non-linear entities into polyhedral convex faces [25] or points [13]. These algorithms do not use the exact representation of the object. Using the point-set model instead of exact representation does not yield the correct geometry of the MAT [14] unless optimization techniques are used. When free-form faces are discretised into polyhedral convex faces, it must be noted that additional effort is required in trimming and post-processing the generated MAT to be in conformity with the topology of the original free-form object. The additional MAT segments will distort any reasoning based on MAT (see Fig. 2(b), where the MAT is substantially different when the exact representation is used (Fig. 2(a))). For finite element applications, such a MAT representation may be sufficient but exact representation of the part has to be used

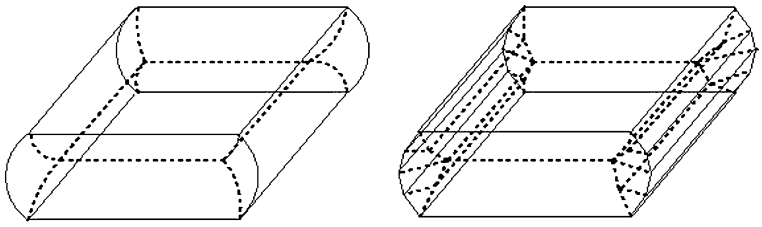

(a) (b)

Fig. 2. Effect of discretising boundary on MAT.

to construct the MAT in applications where the geometry of the part has to be reconstructed from the MAT [10].

Using the exact representation of the part for constructing the MAT eliminates the need for additional processing required to eliminate the artificial segments that may arise due to the discretisation of the curved entities into polyhedral entities [16].

To the best of the knowledge of the authors, no algorithm thus far has used the exact representation of a free-form object to generate the MAT. Construction of the MAT of CSG objects (obtained by boolean combinations of primitive objects such as cuboid, cylinder) has been addressed in [19]. These objects will involve non-linear curves and surfaces. However, these are restricted to quadric curves and surfaces. Some higher order curves can result due to intersections. The procedure outlined involves construction of Voronoi surfaces (to identify equidistant points) for each pair of boundary entities, and trimming these Voronoi surfaces by other Voronoi surfaces. The nature of surfaces in the primitive solids are used to simplify the computation in constructing the Voronoi surfaces to solution of algebraic equations but the trimming of these Voronoi surfaces is non-trivial. No implementation results are provided.

In this paper, the problem of generating a MAT for solids with free-form curved entities, that are obtained by extrusion or revolution about an axis of a profile, has been addressed. The 3D MAT is generated from the 2D MAT of the profile being extruded or revolved. The 2D MAT is obtained by a tracing algorithm described in [28]. The algorithm proposed uses the exact representation of the part and generates an approximation (to within a defined tolerance) of the MAT that is represented by rational spline curves and surfaces. It is shown that the MAT points of the profile face is sufficient to determine the topology and geometry of the MAT of the above class of solids. The algorithm is applicable to objects generated through multiply-connected planar profile face also. The remainder of this paper is structured as follows: Next section presents terminology used in the paper. Overview of the algorithm is presented in Section 3. Some theoretical results that form the basis of the algorithm are derived in the subsequent section. Details of the algorithm are presented next followed by results of implementation and a discussion of the results and the algorithm. The paper concludes with a discussion on the use of the proposed algorithm to handle general solids.

2. Preliminaries

2.1. Terminology

Start(End) Profile Plane (SPP(EPP)). The plane containing the profile at the start (end) of the extrusion or revolution is referred to as the Start(End) Profile Plane. Without loss of generality in the remainder of the paper it is assumed that the SPP is the *XY*-plane at origin.

Profile edge. Object edges in the profile plane are called profile edges. Edges in the SPP are called start profile edges (SPE) and in EPP, they are called end profile edges (EPE). In general, profile edge implies SPE unless otherwise stated.

Profile face. Profile face is a closed loop of profile edges. It can also be multiply-connected. Profile face at SPP is called start profile face (SPF) and that at EPP is called end profile face (EPF). In general, profile face implies SPF unless otherwise mentioned.

In the remainder of the paper the profile face is assumed to lie in *xy*-plane. In the case of extruded solids the profile is extruded along the *z*-axis to obtain the solid, and in the case of solids of revolution, the profile is revolved about the *y*-axis. The profile face is assumed to not contain the axis of revolution. The span of revolution is assumed to be less than 360°. Handling solids of revolution without profile faces (span of revolution equal to 360°) is discussed later.

Extruded (Revolved) face. The face formed by extruding (revolving) a profile edge is called an extruded(revolved) face. This face is bound by profile edges from both profile planes in one direction and straight lines (circular arcs) in the other direction.

Ruling. The straight line in the extruded face formed by a point on the profile edge is called a ruling.

Parallels and meridians. In a solid of revolution, the circles described by the points on profile edges are called the *parallels* and the various positions of the profile edges are called the *meridians*.

R_{max}. This is the maximum radius value of the MAT on the profile face.

Fig. 3 illustrates some of the terminology used in this paper. Fig. 4 shows the ruling. Fig. 5(b) shows the parallels and meridians.

2.2. Classification of points on 2D MAT

Points on 2D MAT can be classified based on the properties of their maximal disks [27]. A point whose maximal disc touches exactly two separate boundary segments is called *normal point*. Point N (or any point on the line segment (A, E1) excluding the end points A and E1) in Fig. 6(a) is a normal point. Its underlying maximal disk is shown in Fig. 6(b).

A point whose maximal disc touches the domain boundary in three or more separate segments is called *branch point*. Points E1 and F1 in Fig. 6(a) are branch points. Fig. 6(c) shows the maximal disk corresponding to the branch point E1.

A point whose maximal disc touches the boundary in exactly one contiguous set is called an *end point*. Fig. 6(a), shows the end points A, B, C and D. These points touch the boundary at a point and the corresponding maximal disc is of radius zero.

Blum and Nagel [27] view the MAT of a domain as collection of *simplified segments*. A simplified segment is

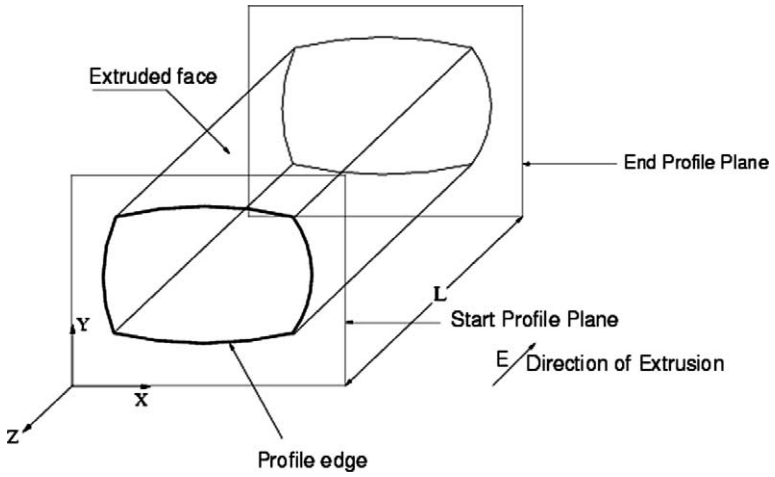

Fig. 3. Terminology for extruded objects.

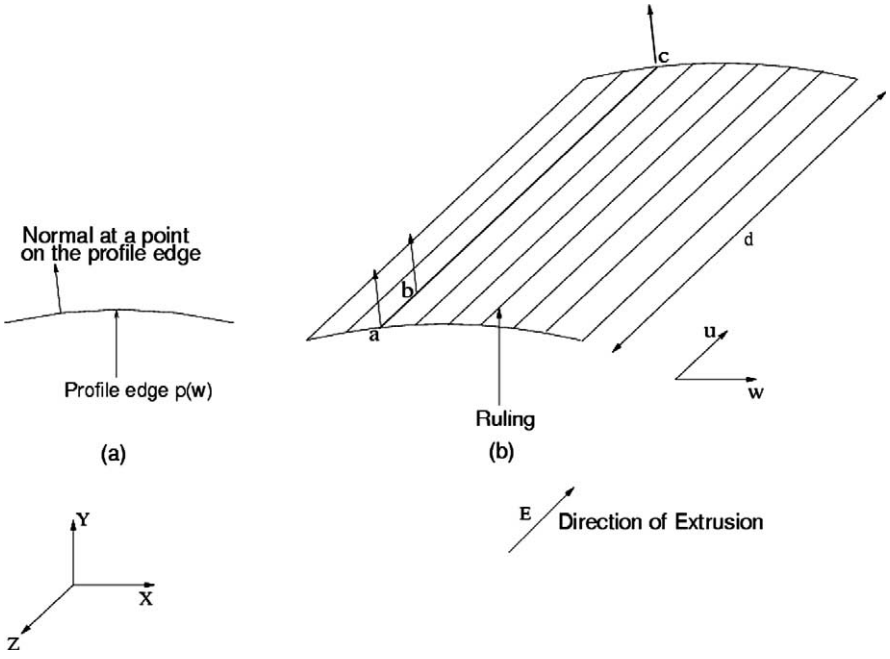

Fig. 4. Normal vector on extruded face.

a set of contiguous normal points bound by either a branch point or an end point [27].

A point of contact with the domain boundary, of the underlying disk of a point on the MAT is called the *footpoint* of the point on the MAT. From the definition of the point types in a MAT, a normal point will have two footpoints (Fp1 and Fp2 in Fig. 6(b)), a branch point will have three or more (Fp1, Fp2, and Fp3 in Fig. 6(c)) and an end point will have one or more footpoints.

2.3. Classification of points on 3D MAT

The various elements that generally comprise the 3D MAT have been defined by Sherbrooke et al. [17] and

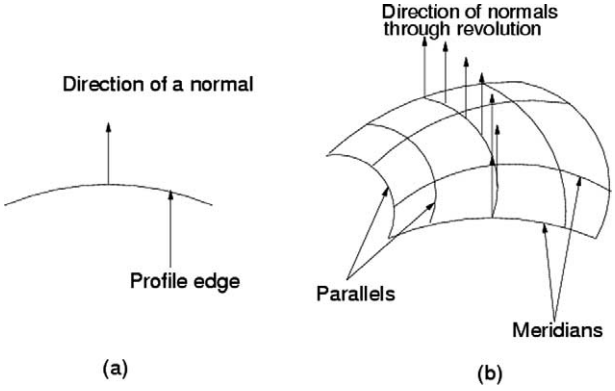

Fig. 5. Normals at the surface of revolution.

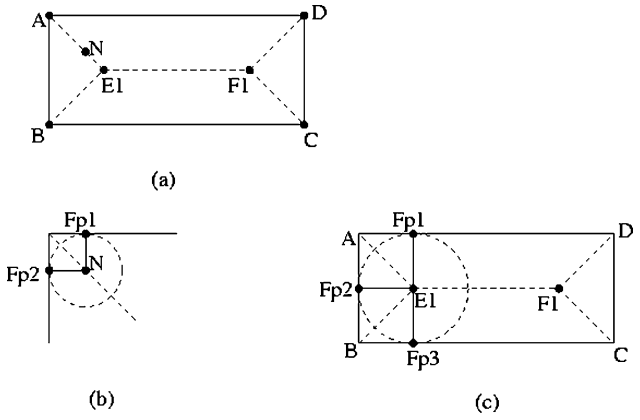

Fig. 6. Classification of points on 2D MAT.

Turkiyyah et al. [14]. These are reproduced here for convenience and are illustrated in Fig. 7.

Touchpoint. A point at which a maximal sphere is tangent to the boundary surface.

Seam. A connected space curve consisting of points that have three touchpoints and are non-manifold. Points on the seam are called *seam points*.

Junction point. A point where the seams intersect.

Seam-End point. These points do not arise from the maximal ball condition of the MAT, but are actually on the limit points of the MAT. A seam-end point generally results when a seam runs into the boundary of the solid. Therefore, vertices with convex edges incident are seam-end points [17].

Skeletal edge. A connected space curve consisting of points whose maximal spheres have a single touchpoint with the surface of the object. A skeletal edge is possible only if a profile edge contains a point that has a locally maximal positive curvature (LMPC) [28].

Sheet. Sheet is a manifold subset of the MAT which is maximal in the sense that it is connected and bounded only by seams and skeletal edges. A seam corresponds to the intersection of sheets. Alternatively, sheets can be obtained as the connected pieces of the MAT created by dissolving all MAT connections across seams.

Sheet point. A point in the interior of a sheet. Sheet points have precisely two touchpoints.

Sheet-End point. These points also are among the limit points of the MAT, but whereas a seam-end point is a limit point of seam, a sheet-end point is a limit point of a sheet. All seam points are sheet-end points but all sheet-end points need not be seam points.

Rim. Connected components of sheet-end points are called rims. Convex edges, resulting from the intersection of sheets with the boundary are rims.

From the classification of the points on 3D MAT, any seam point should be equidistant to three boundary segments, any sheet point should be equidistant to two boundary segments and the junction point should be equidistant to four or more boundary segments.

2.4. Conditions for a MAT point

From the definition of the MAT the following two conditions that have to be satisfied by points on a MAT segment can be derived [26,28].

Distance criterion. Any point on a seam (apart from the other points of the MAT) should be equidistant to three different boundary segments. This is equivalent to saying that any point on the simplified segment of MAT in 2D (apart from the terminal points) should be equidistant to two boundary segments [28].

Curvature criterion. In 2D, for free-form boundaries, it is shown that [26,28] the radius of curvature of the disk at any MAT point should be less than or equal to the minimum of the local radius of curvature of the boundary segments. In 3D, the radius of curvature of the ball (or sphere) at any point on MAT should be less than or equal to the minimum of the radius of curvatures (reciprocal of the maximum normal curvatures) at the touchpoints of the boundary (This condition is similar to the condition to avoid gouging (cutter interference) when

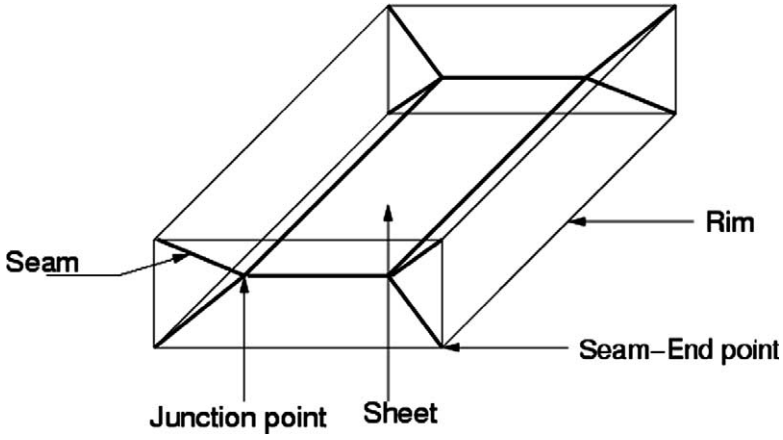

Fig. 7. Classification of points on 3D MAT.

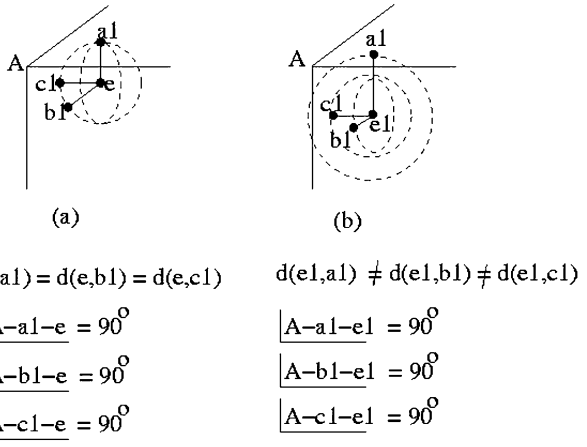

Fig. 8. Distance criterion.

a ball-endmill is used [29]. Otherwise, the ball will not satisfy the *maximal* ball criterion (the ball will pierce the boundary in the same way as the ball-end mill will cause gouging). So the point is no longer a MAT point even though the equidistant criterion is satisfied (one can call such points as bisector points since those points have to be only equidistant [20]. Curvature criterion becomes very important in the case of determining MAT points for free form entities [28]. Without this condition, the generated points belong to a bisector segment and not to a MAT segment. This is also one reason why any approach based on generating bisectors of free-form edge pairs would require additional processing.

In Fig. 8(a) line segments e-a1, e-b1 and e-c1 are normal to the boundary segments and also equal in length. So the *point e* is a point on the MAT. But for the *point e1* shown in Fig. 8(b), even though the line segments e1-a1, e1-b1 and e1-c1 are normal to the boundary segments, they are not equal in length. So *point e1* is not a point on MAT.

Fig. 9 illustrates the curvature criterion. Fig. 9(a) shows that the ball is completely inside the boundary segments which implies that the indicated curvature criterion is fully satisfied and point M becomes a MAT point. Violation of this criterion indicates that the ball does not lie inside the boundary segments completely. The point m in Fig. 9(b) is not a MAT point but it still belongs to the set of bisector points. A point will belong to the MAT only when it satisfies both criteria.

3. Overview of algorithm

The proposed algorithm uses the 2D MAT of the profile (that is extruded or revolved) to construct the 3D MAT of the extruded solid or the solid of revolution. Most of the entities forming the 3D MAT are obtained by applying the same transformation on the 2D MAT as is applied to the profile. The critical task is to identify the limiting entities of the 3D MAT (seam points, junction points, seam and skeletal edges) correctly. The algorithm identifies these from the limiting entities in the 2D MAT (branch points, normal points and points having locally maximum positive curvature) of the profile. This is possible because the two transformations considered (to obtain the solid) have the following characteristics along the span of extrusion or revolution:

- The normal to the extruded/revolved face at a point on the profile face is along the same direction as the normal to the corresponding profile edge at that point.
- The principal curvatures at any point on an extruded (or revolved) face are the curvature at the corresponding point on the profile edge and the curvature at the ruling/parallel, respectively.

These two characteristics are derived for the two types of solids based on their transformation.

The algorithm starts with the 2D MAT on the start profile face (SPF) of the object. The maximum value among the radii of MAT points is then identified. This is then checked against the span of extrusion or revolution to determine whether it is possible to generate the 3D MAT from the 2D MAT.

The junction points in the 3D MAT are first identified using the branch points of the 2D MAT. It is proved that the branch points of the profile faces are sufficient to completely determine the junction points. Identification of junction

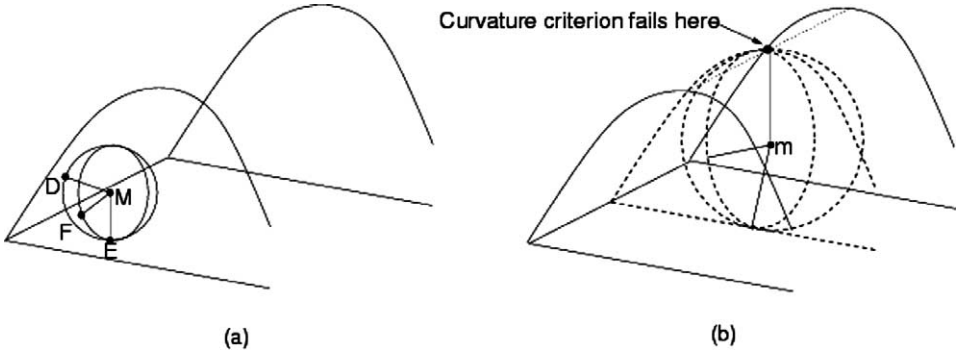

Fig. 9. Curvature criterion.

points using branch points avoids the need to perform a distance check at all seam points and with all faces of the object. This reduces the computational complexity. Points on the seam are then generated using the normal points on the 2D MAT of the profile face (both ends). This is accomplished by transforming the normal point on the 2D MAT of the start profile face and the end profile face. The critical step is the computation of the span of transformation (length of extrusion or the angle of revolution). The span of transformation is computed based on the radius function of the 2D MAT. It is shown that the seam points so obtained satisfy the distance criterion and the curvature criterion. The algorithm therefore, provides a simpler method to obtain the MAT as compared to one based on solution of differential equations (favored by current art [13,17,18]). Simplicity of the proposed method is due to the elimination of complex and computationally expensive numerical procedures to solve the differential equations.

Identification of junction points using the branch points will generate three seams (if the branch point is not a degenerate one). This is because, a non-degenerate branch point will have three MAT segments. Since a non-degenerate junction point will have four seams, the fourth seam is identified next. The fourth seam is obtained by finding the ruling or parallel corresponding to the junction point. The span of the transformation to identify the ruling/parallel is equal to the span between the junction point derived from one profile face and its corresponding junction point derived from the other profile face. This is repeated for all junction points till all the seams associated with each junction point are obtained. Note, however, that a similar procedure can be used to handle degenerate branch points that will produce degenerate junction points and no special procedures are required to handle such cases.

For profiles with free-form entities, 2D MAT segment can terminate at one of the following—a convex vertex, a branch point, the center of curvature of a point with LMPC. An end point of a 2D MAT segment that is not a branch point or a convex vertex, is the center of curvature of a point with LMPC [26,28]. The ruling/parallel corresponding to these limit points in the 2D MAT therefore are the *principal curves* in the notation of Turkiyyah et al. [14]. The maximal spheres corresponding to these points have a single point contact and the centers of such spheres form the skeletal edge. In our procedure, the skeletal edge is obtained directly by transforming the limit point (which is the center of curvature corresponding to point with LMPC in the profile edge) on the 2D MAT.

The algorithm terminates when all the limit points in the 2D MAT have been processed. Interpolation of the seam points generates the seams. Sheets formed by seams between junction points are obtained by transforming the seams and the remaining sheets are obtained using a surface interpolation scheme. Seams and sheets are represented as NURBS curves and surfaces, respectively.

4. Theoretical background

It can be shown that the normal to the extruded/revolved face at a point on the profile face is along the same direction as the normal to the corresponding profile edge at that point. Moreover, it can also be shown that the normal at any other point on the extruded or revolved face is obtained by a similar transformation of the normal at the corresponding point on the profile edge.

Appendix A.1 states the above result as a theorem and provides a formal proof for the same. Theorem 1 follows from the results for parallel transport in differential geometry [31]. However, a formal proof has been derived for the parametric representation of the profile and surface for the sake of completeness.

The significance of the above results is that a footpoint on the 2D MAT when transformed (either by extrusion or revolution) is a potential touchpoint for the 3D MAT with the transformed centre of the disk in the 2D MAT as the centre of the maximal ball.

It has been shown [31] that for a surface of extrusion or revolution, the lines of curvature are the parallels and the meridians. Appendix A.2 presents the derivation of the principal curvatures for the objects of extrusion and also for the surface of revolution represented parametrically for the sake of completeness. Fig. 10 shows the two principal planes (containing the minimal curvature and maximal curvature curves, respectively) at a point p on an extruded surface.

Corollary 1. *The curvature criterion is automatically satisfied at the 3D MAT point obtained by transforming a 2D MAT point on the profile plane*.

Proof for extruded objects. When $k_1 > 0$ (refer Appendix A.2), it implies that maximal positive curvature at any point on the surface of extrusion is the same as that on the corresponding profile edge (given by k). When $k_1 \leq 0$, the curvature criterion is not applicable as it is defined only

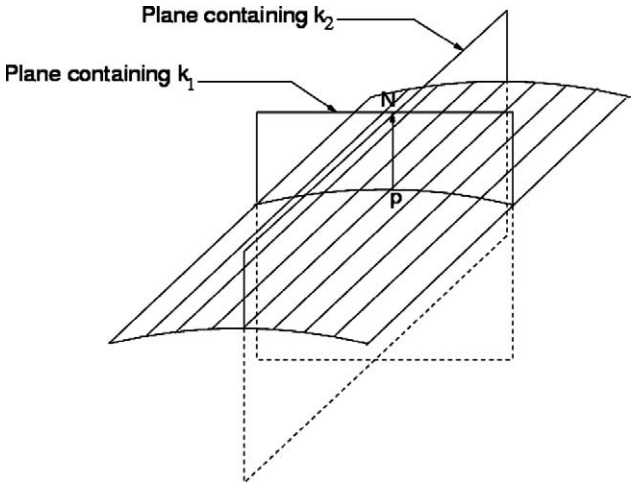

Fig. 10. Geometric interpretation of normal curvature at p.

for regions of positive curvature [26]. Hence the corollary. □

Proof for objects of revolution. Curvature criterion needs to be checked only around regions of maximal positive curvature. Hence only the principal curvature lines on the surface need to be considered. For surface of revolution the principal curvature lines are the meridians (profile) and the parallels, respectively, (Appendix A.2). For a point on the profile, curvature criterion need not be checked against the principal curvature along the meridian as the presence of 2D MAT ensures against violation. For any point on the profile, the curvature is constant along the parallel (both sin θ and x are constant along the parallel (refer Appendix A.2)). For the failure of curvature criterion to happen with respect to the curvature along the parallel, the radius of the maximal ball must be greater than the radius of curvature along the parallel. For a closed domain, this is not possible. Therefore the curvature criterion will not be violated along this principal direction as well. The corollary follows. □

The given theoretical background along with the above Corollary 1 form the basis of the procedure to construct the 3D MAT from the 2D MAT of the profile face.

5. Algorithm details

The algorithm finds the junction and seam points from the points on the 2D MAT of the two profile faces. The seam points here belong to the seam that is either between the junction points and convex vertices or between junction points and other limit points(corresponding to points with maximal curvature) and are identified for each plane. Other limit points of the 3D MAT (corresponding to points with maximal curvature) are then identified. The remaining seams (corresponding to junction points from either profile planes) and the skeletal edges at the limit points are identified. The algorithm terminates when all the limit points in the 2D MAT have been processed and all the seams at each junction point have been determined. The following three main steps in the algorithm are explained in detail.

- Identification of junction and seam points.
- Identification of other limit points.
- Seam identification between junction points.

5.1. Identification of junction and seam points

The junction points corresponding to the branch points in the profile face are identified first. As mentioned earlier, the junction points are obtained by the transformation of the branch points in the 2D MAT of the profile face. In order to do so the span of this transformation is identified first. The span is identified from the radius function of the 2D MAT.

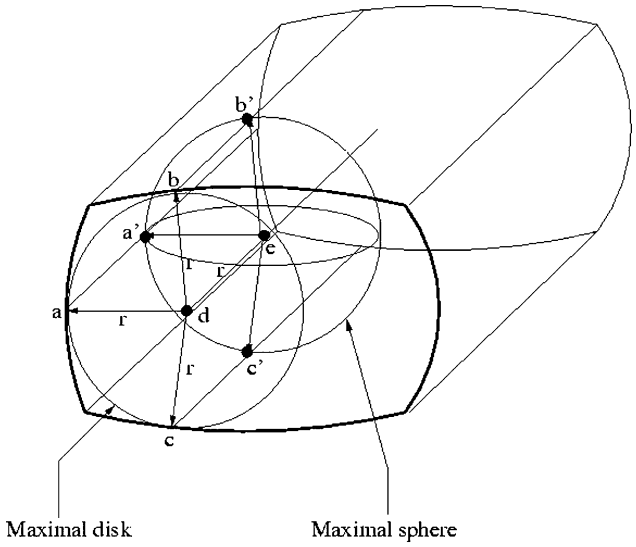

Fig. 11. Junction points using branch points for extruded objects.

When the transformation is extrusion, it is easy to see that the span of extrusion is the radius of the disk at the branch point in the 2D MAT. This is illustrated in Fig. 11.

Point d in the figure corresponds to a branch point of the 2D MAT of SPF and its corresponding footpoints are a, b and c. The maximal disk at the branch point is also shown. Extrusion of the branch point along the extrusion direction by a distance equal to the radius of the disc, results in point e. To prove that point e is indeed a junction point in the 3D MAT, consider the extrusion of the trimmed normals at the three footpoints—ad, bd and cd by the same distance to obtain the points a', b' and c', respectively. Since the extrusion is by the radius of the disk at d, d$'$ is the center of a sphere. By Theorem 1 the touchpoints of this sphere (points a', b', c' and d) on the solid are along the normals to the respective faces. Therefore, the point e is a junction point. It may be noted that the curvature condition is automatically satisfied by Corollary 1. A similar procedure is applicable for branch points in EPF but the extrusion is done along the opposite direction. This procedure avoids the complex distance check.

5.1.1. Span of transformation for revolution

The span of transformation for obtaining the junction points when the solid is obtained by revolving the profile face is derived as follows. Let m be the branch point in 2D MAT (Fig. 12(a)) with its footpoints being a, b and c. Let the branch point m and the normals am, bm and cm be revolved along the path of revolution to obtain the points m', a', b' and c', respectively. From Theorem 1, a sphere centered at m' will have the points a', b' and c' as its touchpoints (Fig. 12(b)). Note that unlike in extruded objects, point m does not become a touchpoint. This is because the normals are moved along the path of revolution (which is not a direction perpendicular to the profile face). For this sphere to be the maximal sphere, it is easy to see

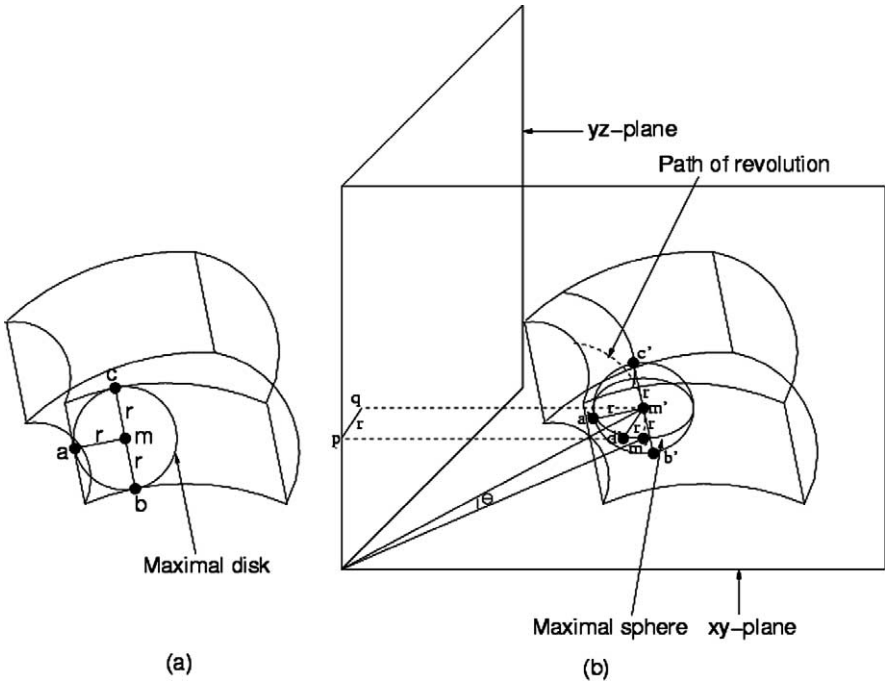

Fig. 12. Required span of revolution.

that the shortest distance between m' and the SPP must be the radius r of the maximal disk at m. We have to therefore determine the span of revolution that ensures that the shortest distance between m' and the SPP is r. Let the point on SPP that is closest to m' be d'. Since the SPP is the XY plane at origin, it follows that, $r = |-x \sin\theta|$ (from Eq. (A.7)), where θ is the angle of revolution. Hence $\theta =$ arc $\sin(r/x)$ is the required span of transformation.

Since r is the radius of a maximal disk (contained in the profile face) and the axis of revolution is not in the profile face, r can never be greater than x.

Proposition 1. *The junction points are completely determined from the branch points of the profile faces at both the profile planes.*

Proof. Let there be a junction point (non-degenerate) which is not corresponding to the branch point. This junction point has by definition four touchpoints on the object. An inverse transformation of the maximal sphere at the junction point by the same span as was used to obtain the junction point would yield a sphere centered at a point on the profile plane. Projection of this sphere on the profile plane will yield maximal disk (by Appendix A.2) that has three footpoints. Hence the corresponding point in the profile face has three equidistant profile edges which has to be a branch point by definition. Hence the proposition □

The above proposition indicates that it is sufficient to use the branch points of both profile faces to identify junction points and this is complete, i.e. there cannot be any other junction point. This is the reason why each seam point is not subjected to the distance check to identify junction points.

5.1.2. Finding seam points

Points on the seam between the junction points identified above are obtained by transforming the normal points in the 2D MAT by spans as identified above. It has been shown that both the distance and curvature criterion are satisfied at the 3D MAT points so obtained. The only thing remaining to be shown is that each point so obtained has exactly 3 touchpoints and therefore, is a seam point.

With reference to Fig. 13, let the point c be a normal point in 2D MAT of the profile face. The corresponding footpoints are a and b and the radius of the disk is r. From Theorem 1, transformation of the two footpoints will yield the touchpoints of a sphere of the same radius centered at a point obtained by transforming the center of the disk. The sphere therefore has three touchpoints and the center of the sphere therefore is a seam point.

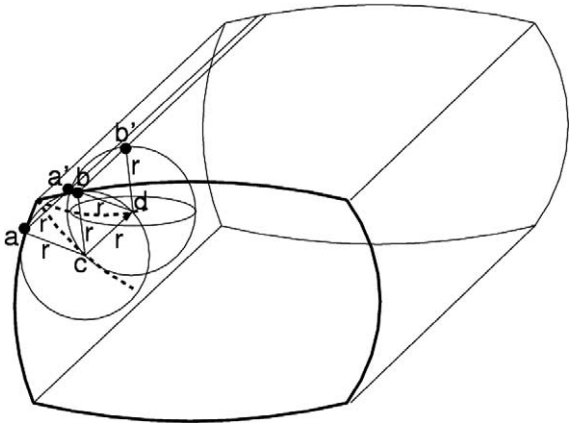

Fig. 13. Seam points using normal points for extruded objects.

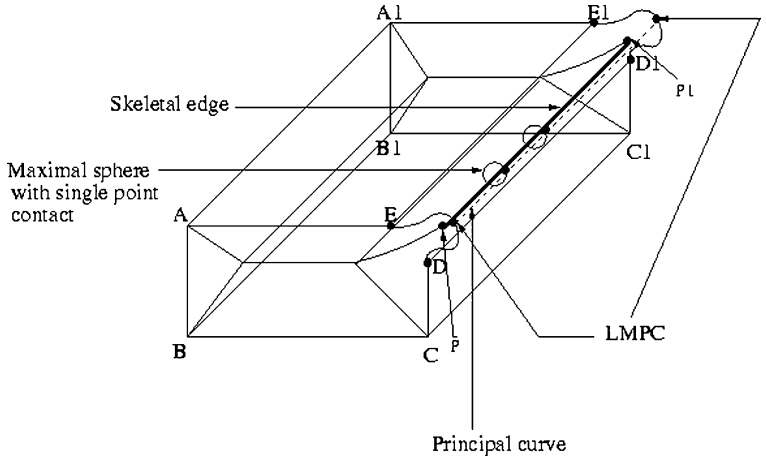

Fig. 14. Smooth case and violation of curvature criterion.

By a mere transformation of normal points of MAT on the profile face, a point on the seam satisfying the distance criterion is obtained.

This process is repeated from the end profile face to generate seam points from the normal points of the MAT on the EPF.

It may be noted that the span of transformation identified above to obtain the junction and seam points also imposes a lower bound on the span of transformation used to obtain the solid. If the distance through which the profile face is extruded is less than $2\times R_{\max}$ (alternately the angle through which the profile face is revolved is less than $2\times \arcsin(R_{\max}/x)$, where x is the corresponding x-coordinate value of that MAT point), then the above procedure to identify the junction points and seam points will not work.

In the case of extruded solids, the sphere centered at the seam point obtained by extruding the normal point will not be maximal only if the other profile face is less than the diameter of this sphere away from the profile face being considered. A similar argument works for the case of revolved solids. It is sufficient to consider $R_{\max}$ because all other disks (and consequently, the spheres) will be smaller.

At the beginning of the algorithm, it is checked if the span of transformation of the solid is more than the respective lower bounds.

As long as the extruded distance is greater than twice the maximum radius of MAT of the profile face, the above procedure identifies non-degenerate junction points. When the extruded distance is equal to $2\times R_{\max}$, the algorithm will generate degenerate junction points and seams. Degenerate cases also arise when the radius value at a branch point becomes the maximum radius value of MAT on the profile face. Similarly, degeneracies happen in the case of objects of revolution if the angle of revolution is equal to the corresponding lower bound.

5.2. Finding other limit points

A 2D MAT segment terminates at one of the following—a convex vertex, a branch point, the center of curvature of a point with LMPC. When the limit point is a convex corner, the convex vertex also becomes a termination point for the 3D MAT. Identifying junction points corresponding to the branch points has been described above. This section describes identifying the entities in the 3D MAT corresponding to the center of curvature of a point with LMPC. In such cases, the maximal disk has a single footpoint on the boundary, i.e. the maximal disk touches the boundary at only one point.

The 3D limit point corresponding to this 2D limit point is obtained as in the other cases by transforming the 2D limit point as described earlier. Similar to the seam between junction points there are skeletal edges between such 3D limit points (obtained from the two profile faces). The skeletal edge is obtained as a ruling (or parallel for solid of revolution) between the limit point identified for the two profile faces (Fig. 14).

The touchpoints corresponding to the points on the skeletal edge are points of extremal maximal normal curvature [14].

5.3. Seam identification between junction points

At this juncture, all the junctions points have been identified but all the seams connected to the junction points have not been identified. Fig. 15(a) shows the junction points q, q', s and s' and the seams (in thick lines) that have been obtained by transforming the branch points and normal points of 2D MAT till now.

The junction points will have only three seams as they are obtained from branch points with three footpoints. The fourth seam is obtained as a ruling (or parallel for solid of revolution) between the corresponding junction points in

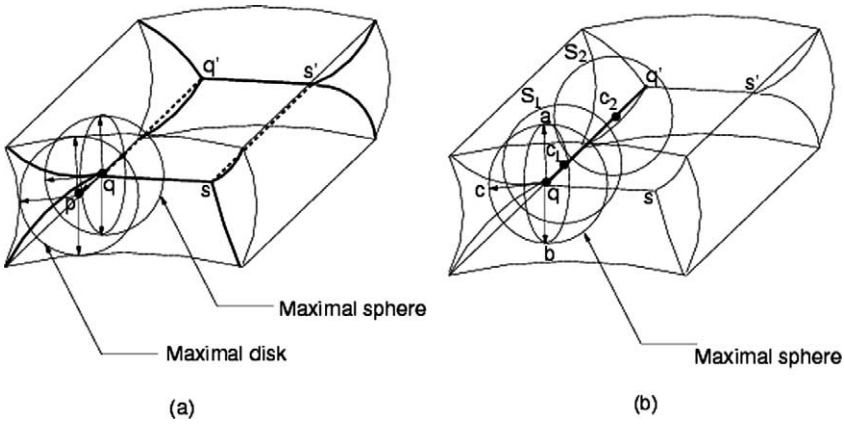

Fig. 15. Seam between junction points.

the two profile faces (Fig. 15(b)). These junction points are then flagged to avoid duplication. If the branch points in the 2D MAT have more than three footpoints then the corresponding junction point will have more than 4 touchpoints. In such cases also the procedure will work and will result in degenerate seams (more than 3 touchpoints).

Proposition 2. *Center of the maximal sphere at a junction point (obtained from a branch point at SPP) generates points on the seam when the sphere is moved along the path of transformation (extrusion or revolution) till it reaches a junction point generated by EPP.*

Proof. At the junction point the sphere will have four touchpoints. Transforming the center of the sphere along the path of transformation of the profile face will reduce the touchpoints by one as the sphere will no longer touch the profile face. As the other three touchpoints will continue to be touchpoints (by Theorem 1), the transformed center will now have three touchpoints only and therefore is a point on the seam. □

6. Results and discussion

The algorithm described has been implemented and this section presents the results obtained for some typical objects. Profile edges are represented as rational B-spline curves, the extruded faces are represented by ruled surface equation and the revolved faces by their corresponding surface of revolution equation. Representation of seams and sheets are discussed later.

MAT obtained for some free-form as well as polygonal extruded objects are shown in Figs. 16–21. The algorithm is able to generate MAT for objects with, complex boundary profiles (Figs. 16 and 17), reflex edges (I-section in Fig. 18), multiply-connected profiles (gear wheel in Fig. 19), polygonal extrusion (machine tool bed, Fig. 20) and smooth edges (Fig. 21). Figs. 22 and 23 show the MAT for objects

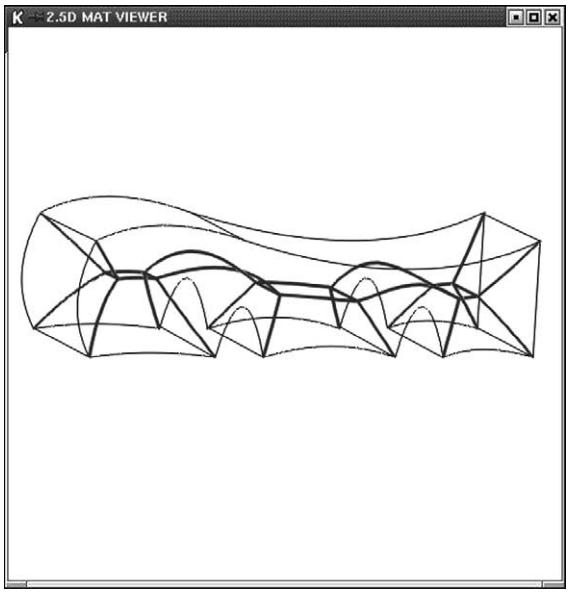

Fig. 16. Test object—extrusion 1 and its MAT.

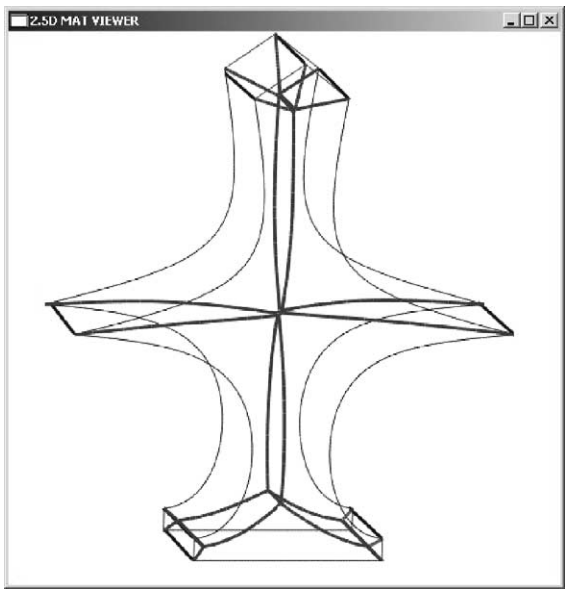

Fig. 17. Test object—extrusion 2 and its MAT.

Fig. 18. MAT of an I-section.

of revolution. Fig. 24 shows that this algorithm can handle objects having degenerate junction points.

Table 1 shows time taken for generating 3D MAT for some of the figures. This time includes the time for generating the MAT on the profile faces. The implementation is on a PIII machine with 256MB RAM.

6.1. Discussion

Accuracy of 3D MAT generated depends on

- the step size used for generating the 2D MAT on the profile faces and
- the definition of the sheets from the seams.

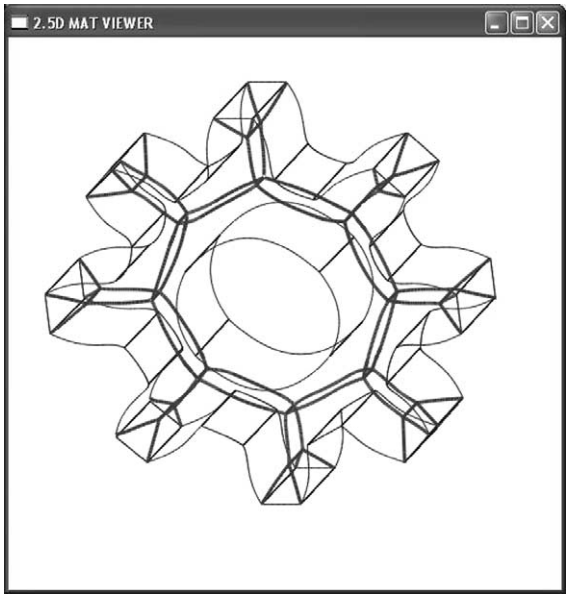

Fig. 19. MAT of gear wheel.

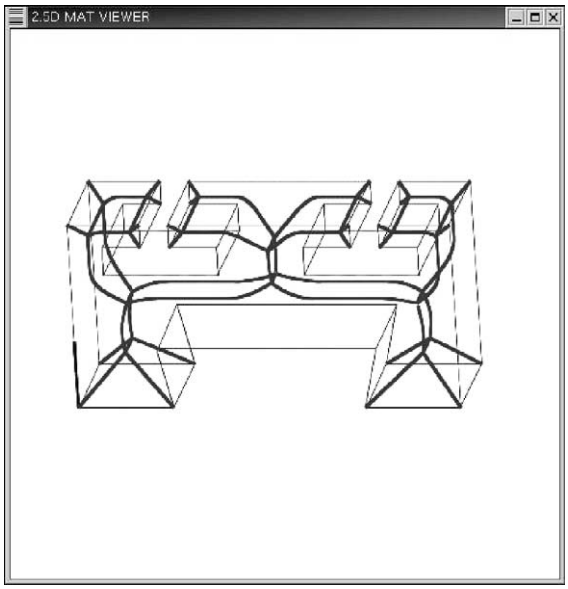

Fig. 20. MAT of a machine tool bed.

Each seam is represented as a rational spline curve. The sheets which have the junctions points as its limits can be represented as surfaces of extrusion or revolution depending on the transformation used to generate the solid. The geometry of the other sheets can be computed since the defining entities (portions of two faces of the solid) of each sheet are known. Assuming a touchpoint on one boundary entity, the corresponding touchpoint on the other boundary entity can be identified numerically and thereby the corresponding MAT point itself. Since the bounding curves of the sheet are known, a suitable surface interpolation scheme can then be used to identify the geometry of that sheet. Fig. 25 shows the mesh of iso-parametric curves on some of the medial surface patches for a test object.

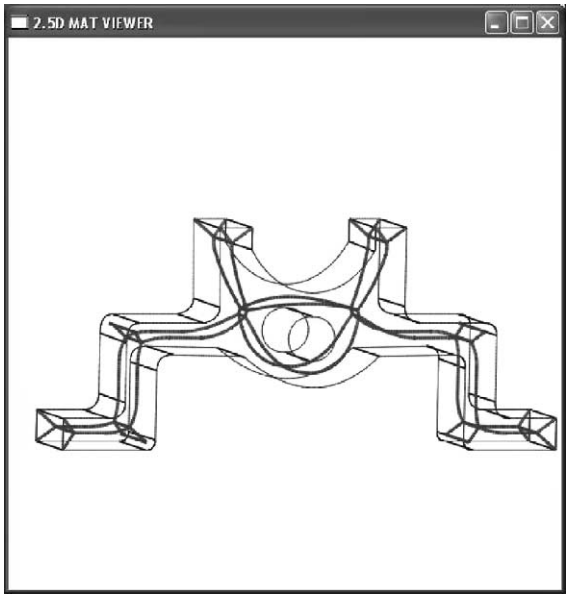

Fig. 21. MAT of a housing bracket.

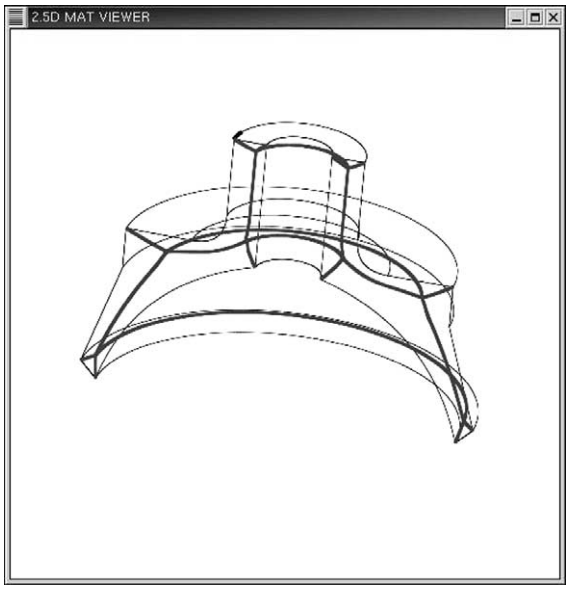

Fig. 22. MAT of universal spider joint.

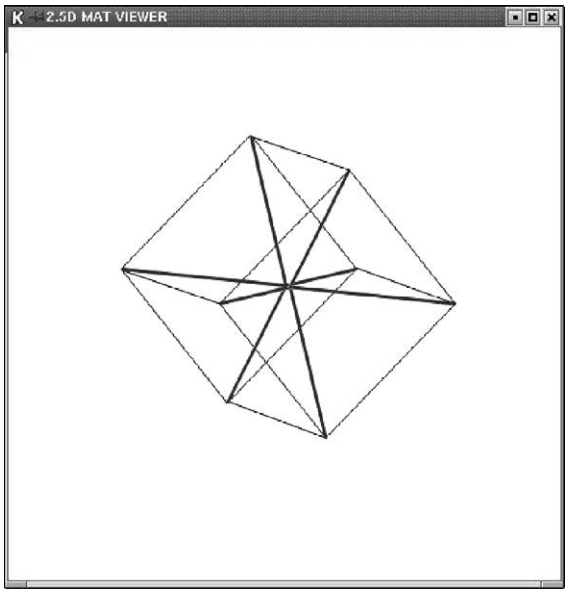

Fig. 24. Object having a degenerate junction point.

The completeness of the algorithm is argued as follows. *Completeness* refers to the generation of all seams in the 3D MAT. By Proposition 1 all junction points are obtained by processing all the branch points in the 2D MAT. Subsequent steps generate all the seams at each junction point. Therefore, all the seams and junction points are determined.

When the solid is obtained by revolving a profile through 360°, the junction points, seams, other limit points and the sheets can be identified as described above. Since the two profile faces are not present in the solid, the 3D entities that correspond to the two faces (convex end points, junction points and seams between junction points that are obtained from a face) will not be present in the final 3D MAT. In this case therefore, seams need not be generated. In the implementation, only the junction points, end points and other limit points in the profile face are identified and these are revolved to form the sheets.

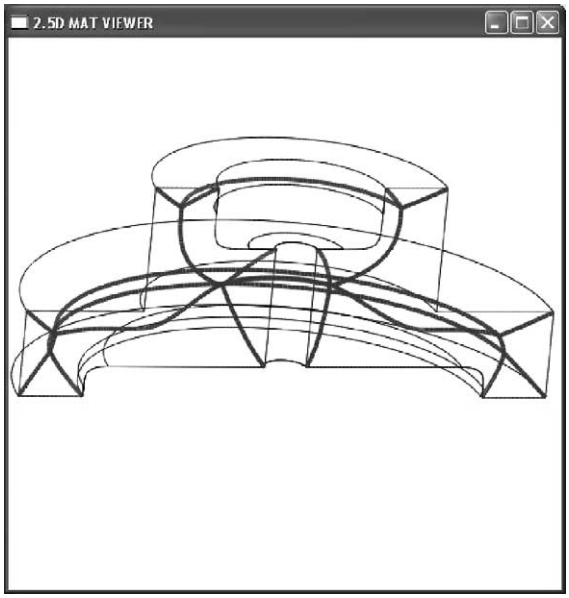

Fig. 23. MAT of a bearing housing.

The proposed algorithm does not use any differential equation for generating seam and junction points. It exploits the nature of the solids under consideration and uses simple transformations to find the MAT entities. Therefore, no complex numerical procedures need to be solved. As the points on MAT determined are based on the definition of MAT, the result will always be correct. The proposed technique is more accurate than differential equation methods as it involves only minimum numerical procedures. Moreover, this method is efficient since distance check is not done on each seam point to identify junction points. It is evident from the Table 1 that the time taken for generating 3D MAT using this algorithm is of the order of seconds whereas other algorithms take time that is in the order of minutes even for polyhedral objects [17]. Time taken for some free form objects can be found in [14] and is in the order of minutes even after incorporating complex optimization techniques.

The approach described in [19] is quite involved as all boundary pairs have to be considered and each Voronoi surface obtained has to be correctly trimmed. Moreover, their approach involves simple algebraic equations only in the case of quadric curves and surfaces. In contrast, our approach exploits the structure of solids (that form

Table 1
Time taken for generation of 3D MAT for typical objects

Figure no.	No. of junction points	Time(in s)
16	12	6
18	12	6
19	32	11

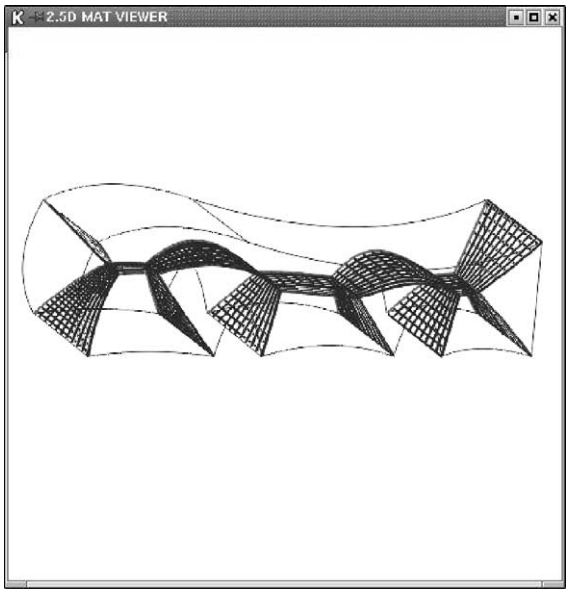

Fig. 25. Mesh of iso-parametric curves on some MAT patches for the test object in Fig. 6.

primitives in general) to obtain a more accurate MAT in an efficient manner. Since the profile can be arbitrary (as long as it is planar) the range of objects handled here is larger than the set of primitives considered in [19].

6.2. Extension to general 3D objects

Even though the scope of the procedures described is restricted to solids of extrusion and revolution, we believe that the results obtained can be used in the construction of MAT of more general solids analogous to the construction of 3D objects by Boolean combination of simple objects. It must be mentioned here that typically all primitives used CSG systems fall in the category of either extruded or revolved solids. Given a general 3D solid that is a combination of two or more solids of extrusion or revolution we discuss the use of the MAT of the primitives to obtain the MAT for the general solid.

Fig. 26(a) shows two extruded objects A and B and their medial surfaces (in bold lines). A general object obtained as a Boolean union of A and B is shown in Fig. 26(b). The MAT of the union of objects could be determined as follows. First the portions of the boundaries of A and B that are not part of the union are identified. The MAT entities

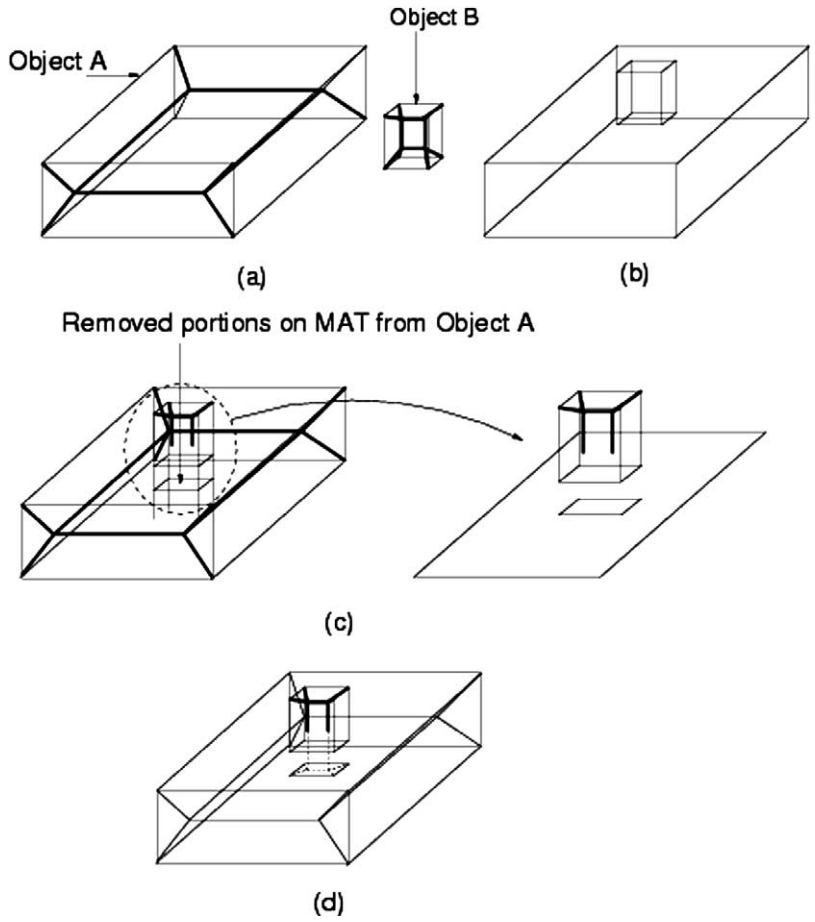

Fig. 26. Medial axis for union of two 3D objects.

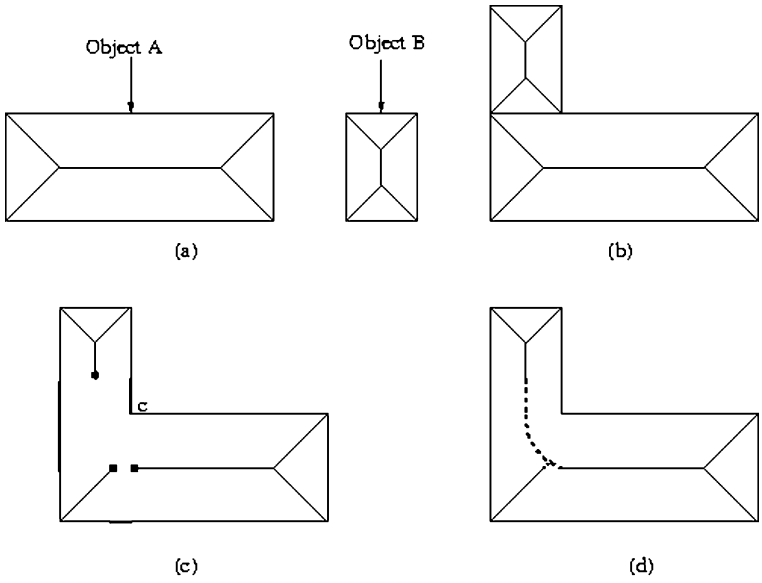

Fig. 27. Medial axis for union of objects.

corresponding to these portions of the boundary are then removed from the 3D MAT of A and B, respectively, (Fig. 26(c)). The portions of the remaining boundaries of A and B for which the MAT points are not available are identified. A tracing procedure in 3D (similar to the 2D tracing procedure in [28]) can now be used to generate the missing MAT entities (shown dotted in Fig. 26(d)). This procedure is likely to be efficient because, the number of domain entities involved are smaller and the points where the tracing has to terminate are also known.

A 2D illustration of the above procedure is shown in Fig. 27 for clarity. Frame (c) in the figure shows the boundary entities(which includes the concave vertex *c*) for which the MAT points have to be determined in bold and the termination points of the MAT for the remainder of the domain is marked with filled dots. The tracing technique has to now only march through the segments shown in bold to identify the missing MAT segments (shown dotted in Fig. 27(d)) that terminate at the points marked in frame (c).

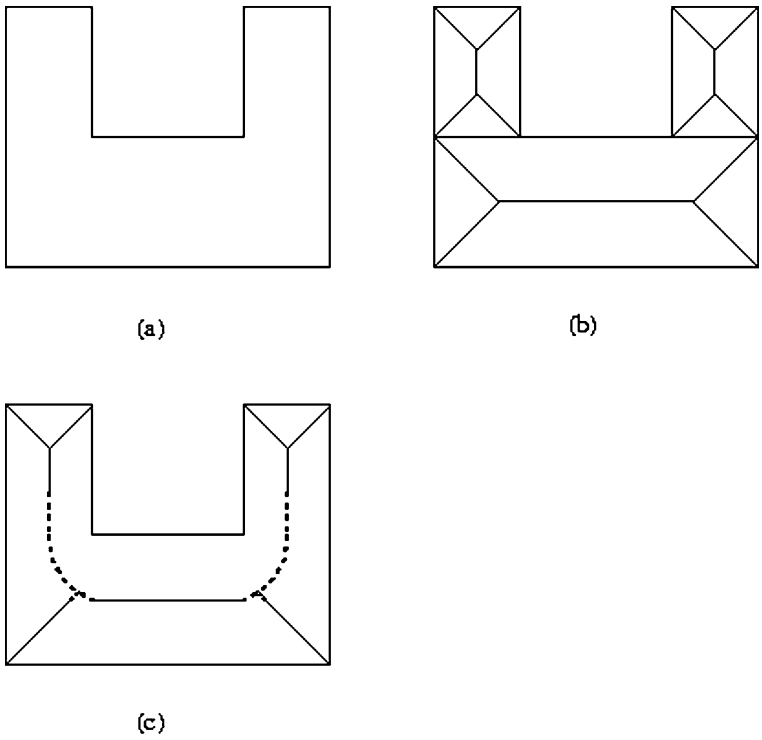

Fig. 28. Medial axis for object obtained using difference operation.

The above idea will work only for an object obtained as union of two objects. In the case of objects that would otherwise involve difference operation, a convex decomposition like approach may be used to identify the simpler objects that on union would yield the object. This is illustrated in the Fig. 28.

7. Conclusions

An algorithm for generating the medial axis transform (MAT) for extruded or revolved 3D objects with free form boundaries has been described. The algorithm generates the MAT by a transformation of points available in the MAT of the profile faces instead of using numerical tracing procedures. Criteria derived from the definition of the MAT are used to generate the points on the MAT and identify the junction points. The algorithm is shown to be robust and correct. Results of implementation on typical solids, including multiply-connected solids have been provided. Extending the idea to handle more general solids has been discussed.

Appendix A. Theory for generating MAT of 2.5D objects

A.1. Normal theorem

Theorem 1. *The normal to the extruded/revolved face at a point on the profile face is along the same direction as the normal to the corresponding profile edge at that point. Moreover, the normal at any other point on the extruded or revolved face is obtained by a similar transformation of the normal at the corresponding point on the profile edge*.

Proof for extruded faces. Let the profile edge be represented by $p(w)=(x(w),y(w),0)$. The normal n and curvature k of the profile edge are given by:

$$n = (-y^w, x^w) \tag{A.1}$$

$$k = (x^w y^{ww} - y^w x^{ww})/((x^w)^2 + (y^w)^2)^{3/2} \tag{A.2}$$

A point on a surface obtained by extruding a profile edge is given by

$$Q(w,u) = [\, x(w) \quad y(w) \quad -du \,] \tag{A.3}$$

where d is the length of the ruling parallel to the negative z-axis.

The normal **N** at any point on the extruded face is given by the cross product of the vectors Q^w and Q^u.

$$\mathbf{N} = Q^w \Lambda Q^u \tag{A.4}$$

where Λ denotes the cross product. Q^t is the partial derivative of Q with respect to t.

Since,

$$Q^w = \begin{bmatrix} x^w & y^w & 0 \end{bmatrix} \quad Q^u = \begin{bmatrix} 0 & 0 & -d \end{bmatrix} \tag{A.5}$$

the normal vector **N** is given by

$$\mathbf{N} = d\begin{bmatrix} -y^w & x^w & 0 \end{bmatrix} \tag{A.6}$$

Comparing the Eqs. (A.1) and (A.6) proves the above theorem (refer Fig. 4(b)). □

Proof for surface of revolution. The surface of revolution $R(w,\phi)$ obtained by revolving the profile edge about the y-axis is given by:

$$R(w,\phi) = \begin{bmatrix} x(w)\cos\phi & y(w) & -x(w)\sin\phi \end{bmatrix} \tag{A.7}$$

Normal on the surface of the revolution is given by the cross product $R^w \Lambda R^\phi$, where $R^w = R^w(w,\phi)$ and $R^\phi = R^\phi(w,\phi)$.

$$R^w \Lambda R^\phi = \begin{bmatrix} -xy^w\cos\phi & xx^w & xy^w\sin\phi \end{bmatrix} \tag{A.8}$$

The normal to the surface at the profile edge is obtained by evaluating the above expression at $\phi=0$. At $\phi=0$, the above equation gives the following:

$$(R^w \Lambda R^\phi)|_{\phi=0} = \begin{bmatrix} -xy^w & xx^w & 0 \end{bmatrix}$$

i.e.

$$(R^w \Lambda R^\phi)|_{\phi=0} = x\begin{bmatrix} -y^w & x^w & 0 \end{bmatrix} \tag{A.9}$$

Also, Eq. (A.8) can be written as:

$$(R^w \Lambda R^\phi)|_{\phi=0} \times \mathbf{Rot\_y}, \tag{A.10}$$

where **Rot_y** is the matrix corresponding to y-axis rotation. Eqs. (A.9) and (A.10) prove the theorem (Fig. 5(b)). □

A.2. Calculation of principal curvatures

For extruded face

The expressions for the prinicpal curvatures determines the values of curvatures at the meridians and parallels. For an object of extrusion, the principal curvatures of a surface $Q(w,u)$ are determined from the equation

$$k_1, k_2 = H \pm \sqrt{(H^2 - K)} \tag{A.11}$$

where H is the mean curvature and K is the Gaussian curvature [31].

The Gaussian curvature K is given by [30]

$$K = \frac{AC - B^2}{|Q^w \Lambda Q^u|^4} \tag{A.12}$$

and the mean curvature is given by [30]

$$H = \frac{A|Q^u|^2 - 2BQ^w \cdot Q^u + C|Q^w|^2}{2|Q^w \Lambda Q^u|^3} \tag{A.13}$$

where $(A\ B\ C) = [Q^w\ \Lambda\ Q^u] \cdot \begin{bmatrix} Q^{ww} & Q^{uw} & Q^{uu} \end{bmatrix}$.

For a surface of extrusion (along u):

$$Q^{ww} = \begin{bmatrix} x^{ww} & y^{ww} & 0 \end{bmatrix}, \quad Q^{uu} = 0, \quad Q^{uw} = 0. \tag{A.14}$$

Therefore,

$$A = d(x^w y^{ww} - y^w x^{ww}), \quad B = 0, \quad C = 0. \tag{A.15}$$

Substitution of A, B, and C gives $K=0$ and

$$H = \frac{A|Q^u|^2}{2|Q^w \Lambda Q^u|^3} \tag{A.16}$$

Simplifying

$$H = k/2 \tag{A.17}$$

where k is the curvature of the profile edge. Hence,

$$k_1 = k, \tag{A.18}$$

$$k_2 = 0. \tag{A.19}$$

For surface of revolution

This is done similar to the derivation for the objects of extrusion

For a surface of revolution $R(w,\phi)$, and mixed partial derivative values area as follows.

$$R^{ww} = \begin{bmatrix} x^{ww}\cos\phi & y^{ww} & -x^{ww}\sin\phi \end{bmatrix} \tag{A.20}$$

$$R^{\phi\phi} = \begin{bmatrix} -x\cos\phi & 0 & x\sin\phi \end{bmatrix} \tag{A.21}$$

$$R^{w\phi} = \begin{bmatrix} -xw\sin\phi & 0 & -xw\cos\phi \end{bmatrix} \tag{A.22}$$

Solving for A, B, and C yields the following

$$A = xx^w y^{ww} - xy^w x^{ww}, \tag{A.23}$$

$$B = 0, \tag{A.24}$$

$$C = x^2 y^w. \tag{A.25}$$

The corresponding Gaussian curvature K and mean curvature H are then obtained from Eqs. (A.12) and (A.13), as

$$\begin{aligned} K &= ky^w/(x((x^w)^2 + (y^w)^2)^{1/2}), \\ H &= k/2 + (y^w/(2x((x^w)^2 + (y^w)^2)^{1/2})), \end{aligned} \tag{A.26}$$

where k is the curvature of the profile edge given by the Eq. (A.2). The prinicipal curvatures are identified using Eq. (A.11).

$$\begin{aligned} H^2 - K &= (k/2 - (y^w/(2x((x^w)^2 + (y^w)^2)^{1/2})))^2, \\ \sqrt{(H^2 - k)} &= k/2 - (y^w/2x((x^w)^2 + (y^w)^2)^{1/2})). \end{aligned} \tag{A.27}$$

Hence,

$$k_1 = k, \tag{A.28}$$

$$k_2 = y^w/x((x^w)^2 + (y^w)^2)^{1/2}). \tag{A.29}$$

k_2 can be simplified as $\sin\theta/x$, where θ is the angle made by the tangent to the profile curve with respect to the x-axis.

References

[1] Blum H. A transformation for extracting new descriptors of shape. In: Dunn W, editor. Models for the perception of speech and visual form. Cambridge: MIT Press; 1967. p. 362–81.

[2] Blum H. Biological shape and visual science (Part I). J Theor Biol 1973;38:205–87.

[3] Baja GS, Thiel E. (3–4)-Weighted skeleton decomposition for pattern representation and description. Pattern Recognit 1994; 27(8):1039–49.

[4] Montanari U. Continuous skeletons from digitized images. J Assoc Comput Mach October 1969;16(4):534–49.

[5] Gursoy HN, Patrikalakis NM. An automatic coarse and finite surface mesh generation scheme based on medial axis transform: part 1 algorithms. Eng Comput 1992;8:121–37.

[6] Armstrong CG. Modeling requirements for finite element analysis. Comput Aided Des July 1994;26(7):573–8.

[7] Ramanathan M. Medial axis transform for the prediction of shrinkage and distortion in Castings, MSc Thesis, Department of Mechanical Engineering, Indian Institute of Science, Bangalore, India.

[8] O'Rourke J. Computational geometry in C. Cambridge: Cambridge University Press; 1993.

[9] Reddy JM, Turkiyyah GM. Computation of 3D skeletons using generalized delaunay triangulation technique. Comput Aided Des 1995;27(9):677–94.

[10] Gelston S, Dutta D. Boundary surface recovery from skeleton curves and surfaces. Comput Aided Geometric Des 1995;12: 27–51.

[11] Wolter FE. Cut locus and medial axis in global shape interrogation and representation, design laboratory Memorandum 92–2, Department of Ocean Engineering, MIT, 1992.

[13] Sheehy DJ, Armstrong CG, Robinson DJ. Shape description by medial surface construction. IEEE Trans Visualization Comput Graphics 1996;2(1):62–72.

[14] Turkiyyah GM, Storti DW, Ganter M, Chen H, Vimawala M. An accelerated triangulation method for computing skeletons of free-form solid models. Comput Aided Des 1997;29(1): 5–19.

[15] Farouki R, Ramamurthy R. Specified-precision computation of curve/curve bisectors. Int J Comput Geometry Appl 1998;8(5–6): 599–617.

[16] Sherbrooke EC, Patrikalakis NM, Brisson E. Computation of the medial axis transform of 3-D polyhedra. Proceedings of the solid modeling and applications'95 1995 pp. 187–199.

[17] Sherbrooke EC, Patrikalakis NM, Brisson E. An algorithm for medial axis transform of 3-D polyhedral solids. IEEE Trans Visualization Comput Graphics 1996;2(1):44–61.

[18] Culver T, Keyser J, Manocha D. Accurate computation of the medial axis of a polyhedron, in Proceedings of the symposium on solid modeling and applications, Ann Arbor, Michigan, 1999, pp. 179–190.

[19] Dutta D, Hoffmann CM. On the skeleton of simple CSG objects. J Mech Des Trans ASME 1993;115:87–94.

[20] Elber G, Kim M. The bisector surface of rational space curves. ACM Trans Graphics January 1998;17(1):32–9.

[21] Elber G, Kim M. Computing rational bisectors. IEEE Comput Graphics Appl 1999;76–81.

[22] Elber G, Kim M. Rational bisectors of CSG primitives. Proceedings of the symposium on solid modeling and applications. Michigan: Ann Arbor; 1999 pp. 159–166.
[23] Lavender D, Bowyer A, Davenport J, Wallis A, Woodwark J. Voronoi diagrams of set theoretic solid models. IEEE Comput Graphics Appl September 1992;69–77.
[24] Lee YG, Lee K. Computing the medial surface of a 3-D boundary representation model. Adv Eng Software 1997;28: 593–605.
[25] Etzion M, Ari Rappoport. Computing Voronoi skeletons of a 3-D polyhedron by space subdivision. Comput Geometry Theory Appl 2002;21:87–120.
[26] Chou JJ. Voronoi diagrams for planar shapes. IEEE Comput Graphics Appl 1995;52–9.
[27] Blum H, Nagel RN. Shape description using weighted symmetric axis features. Pattern Recognit 1978;10:167–80.
[28] Ramanathan M, Gurumoorthy B. Constructing medial axis transform of planar domains with curved boundaries. Comput Aided Des 2003; 35(7):619–32.
[29] Choi BK, Jun CS. Ball-end cutter interference avoidance in NC machining of sculptured surfaces. Comput Aided Des 1989;21(6): 371–8.
[30] Rogers DF, Adams JA. Mathematical elements for computer graphics. New York: McGraw-Hill Publishing Company; 1990.
[31] do Carmo MP. Differential geometry of curves and surfaces. Englewoods Cliffs, NJ: Prentice-Hall, Inc.; 1976.

M. Ramanathan is currently working as a post-doctoral associate in the Department of Computer Science, Technion, Israel. He received his MSc (Engg.) and PhD from the Department of Mechanical Engineering at the Indian Institute of Science, Bangalore, India. He earned a BE degree in Mechanical Engineering from Thiagarajar college of Engineering, Madurai, India. His current research interests include geometric modeling, computational geometry and computer graphics.

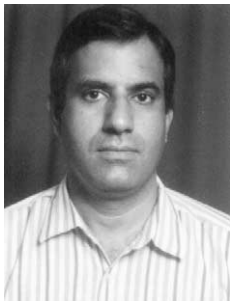

B. Gurumoorthy is currently a Professor in the Centre for Product Design and Manufacturing and the Department of Mechanical Engineering at the Indian Institute of Science in Bangalore, India. He received his BTech in Mechanical Engineering from Indian Institute of Technology, Madras in 1982. He received his ME and PhD in Mechanical Engineering from Carnegie Mellon University, Pittsburgh, USA in 1984 and 1987, respectively. His current research interests are in the areas of geometric modelling, features technology, reverse engineering and rapid prototyping.